Effects of Source Traffic Shaping on MPEG Video Transmission over Next Generation IP Networks

Mohammad F. Alam
Electro-Optics Program, University of Dayton
Dayton, OH 45469-0245, USA

Mohammed Atiquzzaman
Department of Electrical and Computer Engineering, University of Dayton
Dayton, OH 45469-0226, USA

Mohammad A. Karim
Department of Electrical and Computer Engineering, University of Tennessee
Knoxville, TN 37996-2100, USA

Abstract- **The Internet Engineering Task Force (IETF) has defined the Integrated Services model for supporting real-time services. Guaranteed Service is one of these services with firm delay and bandwidth guarantees. Before setting up a Guaranteed Service flow, traffic parameters of the source have to be specified in terms of token bucket traffic descriptors. The source must conform to these descriptors by shaping its traffic. In this paper, we study the effects of a token bucket traffic shaper at the source on the transmission characteristics of Motion Picture Experts Group (MPEG) video streams over the Guaranteed Service. For different types of MPEG video sequences, effects of the shaper parameters on the transmission performance are studied. We develop an analytical model of the traffic shaper, and also carry out numerical simulation of the transmission performance to verify the analytical model. Our study also provides a technique to analyze stored MPEG video sequences to determine the token bucket traffic descriptors that have to be specified during flow set up.**

1. INTRODUCTION

In order to provide quality of service (QoS) guarantee to real-time applications, the Internet Engineering Task Force (IETF) has defined two new services which are collectively called *Integrated Services*: the Guaranteed Service (GS) and the Controlled Load (CL) Service. The Guaranteed Service [1] provides guarantees of bandwidth as well as delay, and is designed to support real-time applications over next generation Internet Protocol (IP) networks. On the other hand, the CL Service [2] provides a service that closely approximates the best-effort service under lightly loaded conditions of the network. Due to the explosive growth of video and multimedia applications, Integrated Services are expected to play a significant role in the next generation corporate IP networks.

Before setting up a Guaranteed Service flow, *traffic parameters of the source have to be specified in terms of token bucket traffic descriptors* [1]. The source must conform to this traffic specification by shaping the generated traffic. In this paper, we discuss a *traffic shaping strategy* for transmission of Motion Pictures Experts Group (MPEG) compressed video streams [3] over the Guaranteed Service.

Previous studies on video traffic shaping primarily focussed on dynamically controlling the data rate of the source [4-6], dynamic adjustment of the characteristics (e.g., bandwidth) of a connection [7-11], and reduction of resource requirements by statistical multiplexing of multiple sources [12,13]. Most of these studies are based on MPEG video transmission over Asynchronous Transfer Mode (ATM) networks, although some studies on MPEG transmission using the Transmission Control Protocol (TCP) over IP networks have been carried out [14]. However, the IETF has specified the User Datagram Protocol (UDP) for transmitting MPEG streams in the Integrated Services model [15]. The connectionless UDP protocol has been chosen for fast transport of real-time streams on IP networks instead of the highly reliable but slow connection-oriented TCP protocol [15]. As far as the authors are aware, *there has not been any systematic study of the traffic shaping requirements for MPEG video transmission* over the Integrated Services.

Recent studies on end-to-end delay of video transmission over Guaranteed Service have assumed either a constant-bit-rate traffic [16] or a simple leaky-bucket traffic shaping [17] at the transmitting end. A leaky-bucket or a constant-bit-rate traffic shaper either fails to utilize the full burst-handling capability of the Guaranteed Service, or can not ensure that the IP packets sent out to the network will be conformant to the traffic specifications. The token bucket, on the other hand, *can transmit traffic bursts up to its allowed limit* which was negotiated at flow setup time while *keeping the traffic flow conformant* to the traffic specifications.

In this paper, we first develop an *analytical model* for studying the effect of the token bucket traffic shaper parameters on delay and buffer requirement for MPEG video transmission using UDP-over-IP transport mechanism. Next, *simulation is used* to calculate delay and buffer requirements using trace data from several different MPEG video sequences and compared with the analytical model. The *simulation results show excellent agreement with the analytical model.* Our method enables an end application to *quantitatively specify the traffic parameters* that are required while setting up an MPEG video stream over the Guaranteed Service.

2. GUARANTEED SERVICE AND MPEG TRANSMISSION

In this section, we discuss the transport of MPEG streams over UDP, the traffic specifications required for setting up an MPEG flow, and the traffic shaping of MPEG streams.

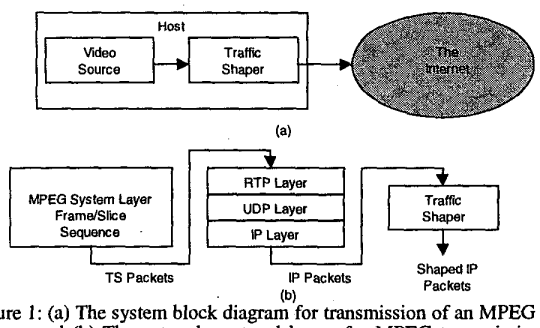

Figure 1: (a) The system block diagram for transmission of an MPEG video stream, and (b) The network protocol layers for MPEG transmission over the Guaranteed Service IP network.

2.1 Transport of MPEG Streams

A real-time stream using any of the Integrated Services on the Internet is established when an end application reserves bandwidth from the network using the Resource ReSerVation Protocol (RSVP) [18]. IETF has defined the Real-time Transport Protocol (RTP) for delivering real-time traffic on IP networks. RTP includes timing information for synchronization during reconstruction as well as feedback on reception quality. The encapsulation mechanism of MPEG video streams in IP packets using the RTP protocol has already been specified [15] by IETF. Figure 1(a) shows the system block diagram for MPEG video transmission, while Fig. 1(b) shows the protocol stack for transporting MPEG video Transport Stream (TS) packets over an IP network. Figure 2 shows a typical IP packet structure carrying an RTP payload.

0-7803-5794-9/99/$10.00 © 1999 IEEE

IP Header IPv4=20 Bytes IPv6=40 Bytes	UDP Header 8 Bytes	RTP Header 12 Bytes	Payload (Variable)

Figure 2: An IP packet structure for real-time MPEG stream transmission using the RTP protocol.

2.2 Traffic Specifications

While setting up a flow over the Guaranteed Service, traffic specifications (TSpec) for the flow have to be specified in advance in terms of a number of token bucket traffic descriptors. The traffic descriptors include: bucket size b, the average (or token generation) rate r and the peak data rate p. Figure 3 shows the token bucket parameters schematically. The TSpec parameters give the end application a way to specify the burstiness present in its generated traffic.

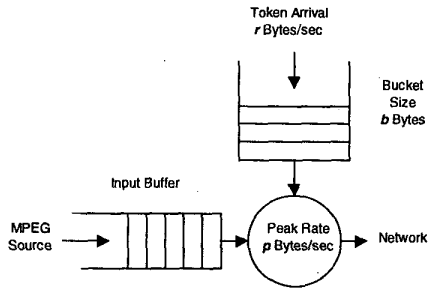

Figure 3: Schematic diagram of the token bucket traffic policing arrangement and the TSpec token bucket paramters (r, b, p) specified in the Guaranteed Service.

2.3 Traffic Shaping of MPEG Streams

MPEG video sequences are arranged into Group of Pictures (GoP). Each GoP contains three different types of frames: Intra (I), Bi-directional (B) and Predictive (P). At the beginning of a GoP, an I-frame is transmitted. After the I-frame, a number of B-frames are transmitted with P-frames inserted between the B-frames. A typical sequence of frames, for example, is IBB-PBB-PBB-PBB. The GoP structure is usually described as *MmNn* where n is the total number of frames in a GoP, and m is the I-P or P-P frame interval. During the transmission of the I-frame, a complete image is transmitted which makes the I-frame much larger in data content than other frames. MPEG video streams are highly bursty in nature with a large burst usually being present at the beginning of each GoP when the I-frame is transmitted. In order to reduce delay and buffer size requirement, it is required that the traffic shaper can transmit a burst of high data rate at the beginning of every GoP period.

A loss-less token bucket is full of tokens at the beginning of each GoP period. Under these conditions, the traffic shaper initially transmits a burst at the peak data rate p for a period determined by the bucket size b, followed by a period of data transmission at a lower rate determined by token generation rate r and input buffer occupancy. Figure 4 shows a typical plot of data transmission rate as a function of time. The period during which data is transmitted at peak rate p is the *burst length*, and the area under the burst length (shaded area in Fig. 4) is the *burst capacity* (or *burst volume*) of the token bucket.

During the initial period of higher data rate, the I-frame is transmitted (completely or partially), while the remaining period is utilized for other frames. A token bucket traffic shaper fully utilizes the burst transmission guarantees provided by the Guaranteed Service in an IP network while ensuring that the generated traffic is fully conformant to the traffic specifications. In a multi-hop transmission, a properly shaped traffic suffers less queuing delays in intermediate network elements, and also suffers from reduced jitter [19]. Also, it is fairly straightforward to simulate the behavior of a token bucket traffic shaper by an easier algorithm, as in [20].

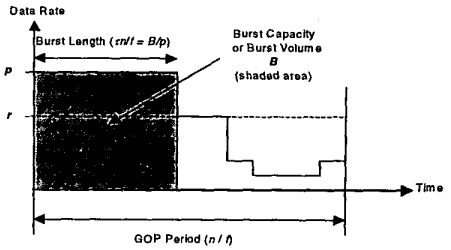

Figure 4: A typical time versus data-rate plot of the token bucket traffic shaper.

3. ANALYTICAL MODEL

In order to calculate the delay and buffer characteristics of the traffic shaper, we assume that the I-frames require a data rate R_I, the B-frames require a data rate R_B, and the P-frames require a data rate R_P. The average data rate, r, for an *MmNn* GoP sequence can be written as

$$r = \frac{R_I + (n - n/m)R_B + (n/m - 1)R_P}{n}. \tag{1}$$

Let us assume that the number of frames per second is f, the peak rate of transmission is p, and the burst volume, which is the area under the peak-rate transmission (at rate p) in the shaper, is B. Also, we define the *normalized burst length* τ as:

$$\tau = \frac{\text{Burst length}}{\text{GOP period}} = \frac{B/p}{n/f} \tag{2}$$

which is the fraction of time the traffic shaper transmits at the peak rate compared to the time taken to transmit one GoP. We also define a *normalized burst volume* β as:

$$\beta = \frac{\text{Burst volume}}{\text{I frame data size}} = \frac{B}{R_I/f} \tag{3}$$

which is the ratio of the burst volume to the I-frame data size in the MPEG video sequence.

3.1 Calculation of Buffer Size

Let us assume that $r_{in}(t)$ is the input instantaneous data rate to the traffic shaper, and $r_{out}(t)$ is the instantaneous output data rate from the traffic shaper at time t (see Fig. 5). We assume that the input buffer is empty at the beginning of each GoP period. The differences between the integrated values of $r_{in}(t)$ and $r_{out}(t)$ represent the instantaneous buffer queue length. This integral reaches a maximum value in each GoP period. The buffer requirement S for a single GoP is given by that maximum value of the integral as

$$S = \max\left[\int_0^t [r_{in}(t) - r_{out}(t)]dt\right]. \tag{4}$$

As explained in the appendix, the buffer size S for a sequence of GoPs can be evaluated from Eq. (4) for the case when the burst length is at least equal to the I-frame transmission time, (i.e., $\tau > 1/n$) as

$$S = K\frac{R_I}{f}\left[1 - \frac{\beta}{\tau n}\right] \tag{5}$$

where we take into consideration the variation of the I-frames from GoP to GoP by introducing the constant K which represents the ratio of maximum to average buffer size so that zero packet loss is achieved. In order to compare different video sequences, we normalize the buffer size S to the average I-frame data size (R_I / f), and define the *normalized buffer size* as $S / (R_I / f)$. This normalized buffer size is used in the discussions in Section 5 where we present results from analysis and simulation.

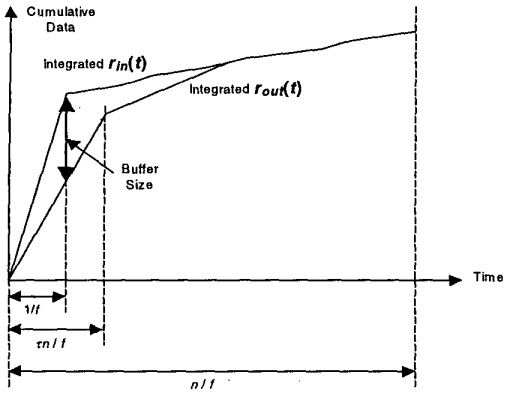

Figure 5: Input data rate $r_{in}(t)$ and output data rate $r_{out}(t)$ integrated to find the maximum difference between the input cumulative data and output cumulative data for calculating the buffer size requirement of the traffic shaper.

3.2 Calculation of Delay

The delays experienced at the shaper buffer by the frames within the same GoP are different for different frames, but is maximum for the I-frame due to its large size. Assuming that the transmission of the I-frame begins exactly at the same instant when the shaper starts its transmission at the peak rate p, the maximum delay experienced by the frames in a GoP is given by the delay experienced by the I-frame. We define this maximum delay as the *GoP delay*. The GoP delay is calculated by the time difference between the end of the arrival of an I-frame and the end of the departure of an I-frame from the traffic shaper. As explained in Appendix, this time difference is the maximum delay experienced by all the frames in a GoP. The GoP delay through the traffic shaper is given by

$$t_{delay} = \begin{cases} \frac{1}{f}\left[\tau n - 1 + R_I \frac{(1-\beta)}{r}\right] & \beta < 1 \\ \frac{1}{f}\left[\frac{\tau n}{\beta} - 1\right] & \beta \geq 1. \end{cases} \quad (6)$$

Equation (6) represents the delay experienced by a single GoP through the token bucket traffic shaper when R_I is the I-frame data rate. When R_I represents the average I-frame data rate for a video sequence comprising of a number of GoP sequences, t_{delay} represents the *average GoP delay*. In order to compare different video sequences, we normalize the average GoP delay t_{delay} to the GoP period $1/f$, and define the *normalized average GoP delay* as $t_{delay}/(1/f)$. We use this normalized average GoP delay also in Section 5 where we present results from both analysis and simulation.

3.3 Token Bucket Burst Parameters

The token bucket parameters are the peak data rate p, the average data rate (or token generation rate) r, and the bucket size b. These parameters (b, r, p) can be related to the burst capacity B and the burst length ($B/p = \tau n/f$) as follows:

$$\frac{b}{p-r} = \tau n / f = B / p. \quad (7)$$

4. SIMULATION

The analytical model presented in Section 3 gives us buffer requirement and delay at the traffic shaper under study. In order to verify the applicability of the analytical model, MPEG trace data from several video sequences have been used as input to a simulation program to find the statistical properties of delay and buffer size. MPEG video sequences contain streams of I, B, and P frames, the bit rates of which vary statistically from frame to frame. Thus the delay and buffer requirements vary for each GoP, and statistical properties of the delay and buffer size need to be studied in order to compare the simulation results with the analytical model. For an MPEG video sequence, all GoPs do not require the same buffer size. We use the maximum buffer requirement of all the GoPs as the required buffer size because a buffer of smaller size will cause data loss at the shaper. For delay, the average delay is a very good indicator of the overall delay performance of the traffic shaper.

A simulation program was written in C, which simulated the behavior of a first-in-first-out (FIFO) queue with the output data transmission rate controlled according to the characteristics of the token bucket traffic shaper. MPEG trace data from several different movie clips [21] were used as input to the simulator. The program takes as input the burst volume and the burst length of the traffic shaper. The shaper parameters are specified in terms of β and τ. The simulation program calculates the delay experienced by each frame, and also keeps track of instantaneous buffer occupancy as it runs. Statistics on delay, jitter and buffer queue length are gathered and saved. The simulation is performed for different ranges of values of β and τ.

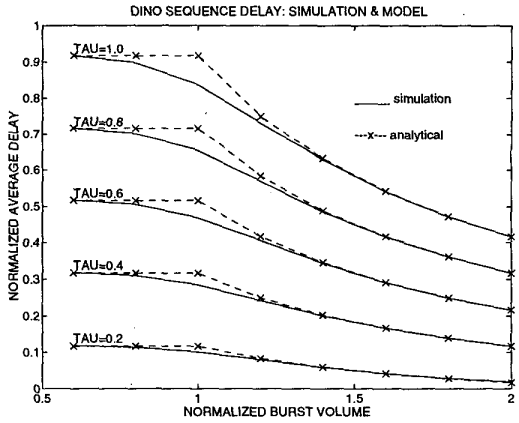

Figure 6: Normalized average delay for a traffic shaper for the DINO sequence as a function of the normalized burst volume specified in the traffic shaper. The solid lines represent simulation results while the broken lines (with × mark) represent analytical results for comparison. Different curves represent different values of τ. Five different curves are plotted for values of τ in the range $0.2 < \tau < 1.0$.

5. RESULTS

First, results from the analytical model developed in Section 3 are presented. Figure 6 shows the normalized average GoP delay t_{delay} as a function of the normalized burst volume β as given by Eq. (6). For brevity, we use the term *delay* to refer to *normalized average GoP delay* defined in Section 3.2, the term *buffer size* to refer to *normalized buffer size* defined in Section 3.1, and the term *burst volume* to refer to *normalized burst volume* β. The broken lines represent the delay from analytical results for the DINO sequence, a sequence from the movie Jurassic Park. The delay is

plotted for τ between 0.2 (short burst-length) and 1.0 (flat, or no burst). For a particular value of τ, the delay is reduced for increased burst volume. For a constant burst volume, increasing τ also increases the delay considerably.

$\tau = 1.0$ represents the case where the traffic shaper transmits at a constant data rate that is equal to the average data rate of the video. The delay for $\tau = 1.0$ is also identical to the delay experienced by a constant-bit-rate transmission as well as a leaky-bucket traffic shaper, since the delay is calculated based on the delay of the I-frame. The traffic shaping delay has been neglected in [17] where end-to-end delay for a network has been calculated based on a leaky-bucket traffic shaper, although the delay experienced by an MPEG stream through a leaky-bucket traffic shaper is comparable to the end-to-end delay. For example, the curve for $\tau = 1.0$ in Fig. 6 shows significant delay through the traffic shaper which is comparable to end-to-end-delays calculated in [17]. Figure 6 also shows that significant reduction in delay can be obtained by choosing a lower value of τ while keeping the burst capacity B constant, i.e., by increasing the peak rate of transmission in the traffic.

Simulation results are presented in Fig. 6 in solid lines where the normalized average delay is shown for the same DINO sequence. Comparing the analytical model results with the simulation results, we observe that there is excellent agreement between the model and the simulation results for delay. The analytical model result for delay represents the delay experienced by a GoP of average GoP size. Thus, the statistical variations of the GoP sizes and frame sizes cause the simulation result curves to become smoother than the analytical results. This can explain the deviation of the analytical results from the simulation results around $\beta = 1$ in Fig. 6.

Figure 7 shows the normalized buffer size requirement as a function of the normalized burst volume for various values of τ as given by Eq. (5) for the same DINO sequence as in Fig. 6. The broken lines represent analytical results. In Fig. 7, for a constant burst-length, the buffering requirement is reduced for increased burst volume of the shaper due to the fact that the buffer size requirement is determined by the difference between the data rates at the input and output of the traffic shaper. For a constant burst volume, decreasing the value of τ also decreases buffer size requirement because of the higher initial data rate with smaller values of τ.

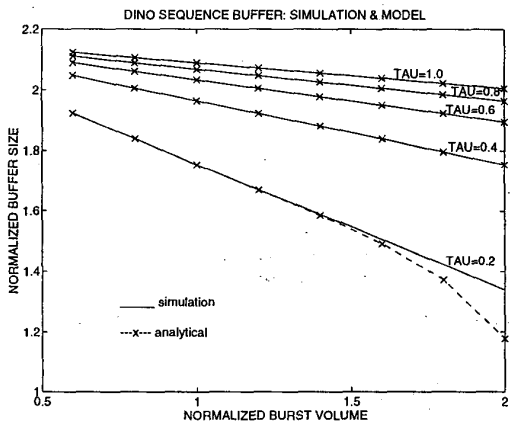

Figure 7: Normalized buffer size for a traffic shaper for the DINO sequence as a function of the normalized burst volume specified in the traffic shaper. The solid lines represent simulation results while the broken lines (with × mark) represent analytical results from for comparison. Different curves represent different values of τ. Five different curves are plotted for values of τ in the range $0.2 < \tau < 1.0$. The solid and broken lines overlap completely for $\tau = 0.4, 0.6, 0.8$ and 1.0.

Simulation results for buffer size are shown in Fig. 7 in solid lines for the same DINO sequence. Excellent agreement between analytical results and numerical simulation is observed for the buffer size.

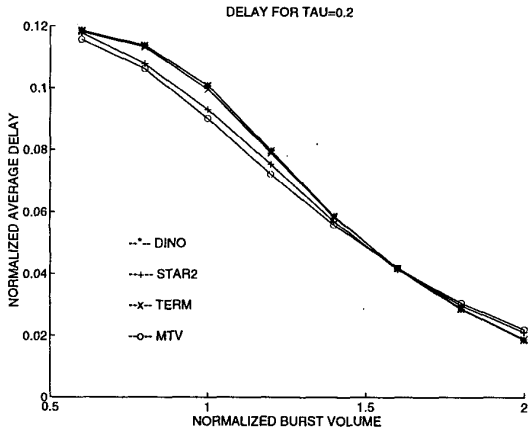

Figure 8: Normalized average delay of four different video sequences as a function of normalized burst volume for the case $\tau = 0.2$. The sequences are DINO(*), STAR2(+), TERM(x), and MTV(o).

In Fig. 8, we compare the simulation results for delay as a function of the burst volume for four different video sequences: DINO (Jurassic Park), STAR2 (Star Wars), TERM (Terminator 2) and MTV. The burst length for all four sequences is set for $\tau = 0.2$. Average delay in each sequence is normalized to unit GoP period while the burst volume is normalized to the average I-frame data size of each of the respective sequences. The close match between four different types of video sequences in Fig. 8 suggests that normalized delay and normalized burst volume are related by a curve which is almost identical for a wide range of video sequences. This general characteristic of the shaper parameters can be effectively utilized for specifying the shaper parameters for a given delay and vice versa. Figure 9 compares the delay for $\tau = 0.6$ for the same four video sequences as in Fig. 8. Close match between different video sequences is also observed in Fig. 8. Although both Figs. 8 and 9 show similar characteristics, the delay ranges are different for the two cases. In Fig. 9, delay is longer due to the higher value of τ chosen compared to Fig. 8.

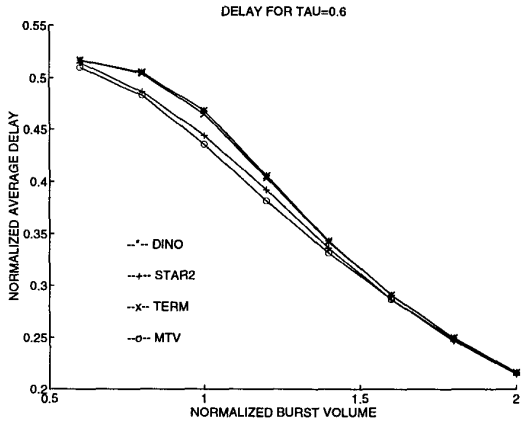

Figure 9: Normalized average delay of four different video sequences as a function of normalized burst volume for the case $\tau = 0.6$. The sequences are DINO(*), STAR2(+), TERM(x), and MTV(o).

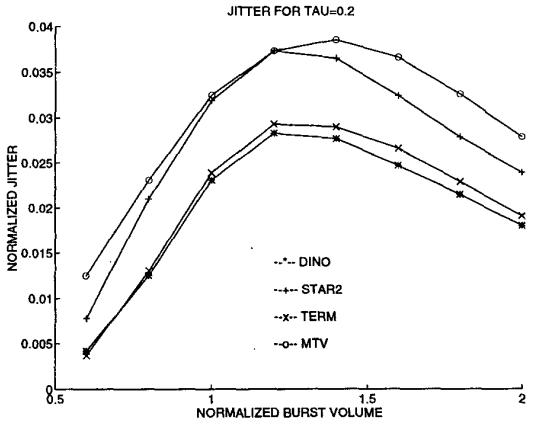

Figure 10: Normalized jitter of four different video sequences as a function of normalized burst volume for the case τ = 0.2. The sequences are DINO(*), STAR2(+), TERM(x), and MTV(o).

The simulation program also gathers information about delay variation (jitter). Since the standard deviation of delay is a good measure of jitter, we denote the standard deviation of normalized average GoP delay as *jitter* for conciseness. In Fig. 10, jitter is plotted as a function of the burst volume for τ = 0.2 for the same four video sequences as in Figs. 8 and 9. The jitter can be seen to increase, reach a maximum, and then decrease with increasing normalized burst volume. In Fig. 11, jitter is plotted for τ = 0.6 for the same four video sequences as in Fig. 10. Figure 11 shows the same characteristics as in Fig. 10 although the range of the jitter scale is different in the two figures.

In Fig. 12, for τ = 0.2, we compare the simulation results for the normalized buffer requirement for the same four video sequences as in Fig. 11 as a function of the normalized burst volume. Wide variation in the normalized buffer requirement is observed for different types of video sequences. In Fig. 13, the buffer requirements for the four video sequences are compared where τ is chosen as 0.6. Again, a wide variation in the normalized buffer size is observed for different video sequences. These variations in buffer size suggest that careful attention is required for choosing the proper buffer size for a particular video sequence, since buffer overflow may cause loss of frames.

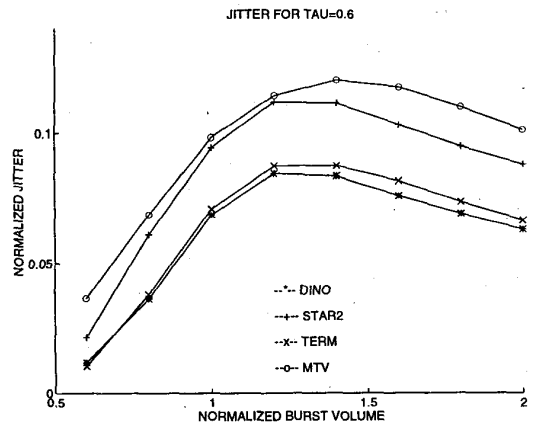

Figure 11: Normalized jitter of four different video sequences as a function of normalized burst volume for the case τ = 0.6. The sequences are DINO(*), STAR2(+), TERM(x), and MTV(o).

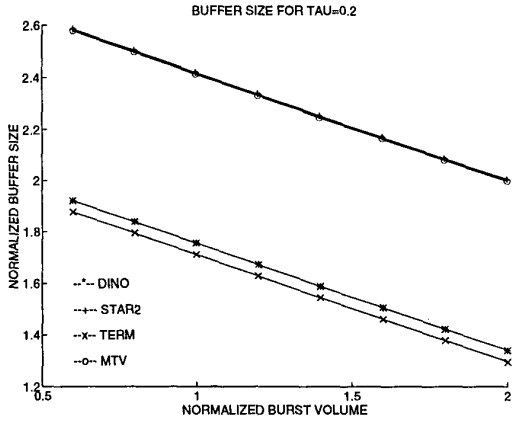

Figure 12: Normalized buffer size of four different video sequences as a function of normalized burst volume for the case τ = 0.2. The sequences are DINO(*), STAR2(+), TERM(x), and MTV(o).

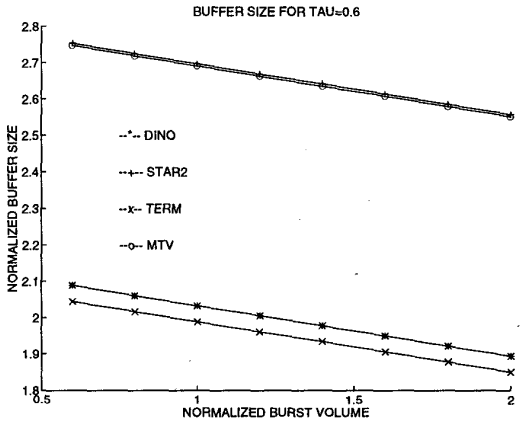

Figure 13: Normalized buffer size of four different video sequences as a function of normalized burst volume for the case τ = 0.6. The sequences are DINO(*), STAR2(+), TERM(x), and MTV(o).

Real-world applications of the results may include finding the proper token bucket parameters (b, r, and p) when a delay is specified. For a given delay, we can choose a value for the burst length τ from a narrow range of values. For example, delay varies between 0.02 and 0.12 for τ = 0.2 in Fig. 8. After specifying τ, the burst volume B can be calculated from Figs. 12 and 13. Then, the token bucket size b and the peak rate p can be calculated using Eq. (7). The token generation rate is calculated from the maximum GoP data size. The maximum GoP data sizes and the average I-frame data sizes for the four sequences are listed in Table I.

Table I. Normalization factors for the four different video sequences.

Sequence	Largest GoP data size (bits)	Average I-frame data size (bits)
DINO	10166368	55076
TERM	8068200	37388
MTV	18231552	69862
STAR2	7052696	44012

6. CONCLUSION

In this paper, we have *analyzed the characteristics of a token bucket traffic shaper* for efficient MPEG video transmission over the Guaranteed Service. The study shows how a token bucket traffic shaper can effectively control the transmission rate so that it

is conformant to the negotiated traffic specification between the user and the network, while fully utilizing the allowed burst-handling capability of the Guaranteed Service.

The results also indicate that for larger burst volumes specified during flow setup, the average delay and buffer size are reduced. Reducing the burst length while keeping the burst volume constant reduces the delay and buffer size requirements at the shaper. Our study also shows that the delay as a function of the burst volume of the token bucket traffic shaper is nearly identical for different video sequences. This characteristic of the traffic shaper can be utilized for choosing appropriate traffic shaper parameters. Jitter has been found to first increase, reach a maximum and then decrease with increase in burst volume for different types of video sequences. Our study further reveals that the buffer size requirement varies widely for different types of video sequences.

Results from this study *can be utilized for specifying suitable traffic specification (TSpec) parameters* that are required while setting up a flow for transmission of stored MPEG video sequences over the Guaranteed Service.

APPENDIX

Eliminating B from Eqs. (2) and (3), we get,

$$p = \frac{\beta R_I}{\tau n} \tag{A.1}$$

From Fig. 5, the buffer requirement reaches its maximum value at the instant $t = 1/f$, provided that $R_I > p > R_P > R_B$. Under this assumption, which is usually true for a GoP, the required buffer size can be written as,

$$S = (R_I - p)/f = (R_I/f)\left[1 - \frac{\beta}{\tau n}\right] \tag{A.2}$$

where Eq. (A.1) is used to arrive at the last step. Here, the buffer size represents the average buffer size. However, we need to multiply this buffer size by a constant K to arrive at Eq. (5) such that K represents the ratio of the maximum-to-average buffer size. The value of K is computed from MPEG trace data.

For $\beta \geq 1$, an I-frame is completely contained inside the burst volume of the shaper. A complete I-frame arrives at the input buffer of the shaper at time $t = 1/f$, and leaves the shaper at time $t = R_I/fP$. Hence, the delay (for the case $\beta \geq 1$), which is the time difference between the arrival and the departure of the end of the I-frame, is given by

$$t_{delay} = \frac{R_I}{fp} - \frac{1}{f} = \frac{1}{f}\left[\frac{\tau n}{\beta} - 1\right], \qquad \beta \geq 1 \tag{A.3}$$

where Eq. (A.1) is used for eliminating R_I. When $\beta < 1$, a complete I-frame is not contained inside the burst volume of the shaper. The burst length (B/p) can also be written as ($\tau n / f$) from definition of τ (Eq. 2). Let us assume that the complete I-frame is transmitted at rate p for the burst length, and also transmission at the average rate r is required for an additional duration of time t'. Thus, the total amount of data transmitted is equal to the data size of the I-frame, and can be written as the sum of the data transmitted at rate p and at rate r as,

$$p\frac{\tau n}{f} + t'r = \frac{R_I}{f} \tag{A.4}$$

from which we get

$$t' = \frac{R_I}{f}\frac{(1-\beta)}{r} \tag{A.5}$$

where b and p are eliminated using Eqs. (A.1) and (3). The total delay for the case $\beta < 1$ can thus be written as the burst length plus t' minus the time of arrival of the I-frame as,

$$t_{delay} = \left(\frac{\tau n}{f} + t'\right) - \frac{1}{f}, \qquad \beta < 1 \tag{A.6}$$

which can be rewritten using Eq. (A.5) as,

$$t_{delay} = \frac{1}{f}\left[\tau n - 1 + R_I\frac{1-\beta}{r}\right], \qquad \beta < 1. \tag{A.7}$$

REFERENCES

[1] S. Shenker, C. Partridge, and R. Guerin, "Specification of guaranteed quality of service," Internet Engineering Task Force, RFC 2212, September 1997.

[2] J. Wroclawski, "Specification of the controlled-load network element service," Internet Engineering Task Force, RFC 2211, September 1997.

[3] The MPEG family of standards includes MPEG-1, MPEG-2 and upcoming MPEG-4, formally known as ISO/IEC-11172, ISO/IEC-13818 and ISO/IEC-14496.

[4] Y.S. Saw, P.M. Grant, J.M. Hannah, and B. Mulgrew, "Video rate control using a radial basis function estimator for constant bit-rate MPEG coders," *Signal Processing: Image Communication*, vol. 13, no. 3, pp. 183-199, 1998.

[5] K.T. Choi, S.C. Chan, and T.S. Ng, "Perceptual based rate control scheme for MPEG-2," *1998 IEEE International Symposium on Circuits and Systems*, vol. 5, pp. V-546-V-548, Monterey, CA, USA, May 31-June 3, 1998.

[6] S. Lee, M.S. Pattichis, and A.C. Bovik, "Rate control for foveated MPEG/H.263 video," *1998 IEEE International Conference on Image Processing*, vol. 2, pp. 365-368, Chicago, IL, USA, October 4-7, 1998.

[7] J.S. Kim and J.K. Kim, "Adaptive traffic smoothing for live VBR MPEG video service," *Computer Communications*, vol. 21, no. 7, pp. 644-653, 1998.

[8] W. Zhu, Y. Wang, and Y.Q. Zhang, "Jitter smoothing and traffic modeling for MPEG-2 video transport over ATM networks," *International Journal of Imaging Systems and Technology*, vol. 9, no. 5, pp. 332-339, 1998.

[9] D.H.K. Tsang, B. Bensaou, and Sh.T.C. Lam, "Fuzzy-based rate control for real-time MPEG video," *IEEE Trans. Fuzzy Systems*, vol. 6, no. 4, pp.504-516, 1998.

[10] J.D. Salehi, Z.L. Zhang, J. Kurose, and D. Towsley, "Supporting stored video: Reducing rate variability and end-to-end resource requirements through optimal smoothing," *IEEE/ACM Trans. Networking*, vol. 6, no. 4, pp. 397-410, 1998.

[11] X. Wang, S. Jung, and J.S. Meditch, "Dynamic bandwidth allocation for VBR video traffic using adaptive wavelet prediction," *IEEE International Conference on Communications*, vol. 1, pp. 549-553, Atlanta, GA, USA, June 7-11, 1998.

[12] B.N. Bashforth and C.L. Williamson, "Statistical multiplexing of self-similar video streams: Simulation study and performance results," *1998 6th International Symposium on Modeling, Analysis and Simulation of Computer and Telecommunications Systems*, pp. 119-126, Montreal, Canada, July 19-24, 1998.

[13] P. Cuenca, B. Caminero, A. Garrido, F. Quiles, and L. Orozco-Barbosa, "QoS and statistical multiplexing performance of VBR MPEG-2 video sources over ATM networks," *1998 11th Canadian Conference on Electrical and Computer Engineering*, vol. 1, pp. 33-36, Toronto, Canada, May 24-28, 1998.

[14] S. Jacobs and A. Eleftheriadis, "Streaming video using dynamic rate shaping and TCP congestion control," *Journal of Visual Communication and Image Representation*, vol. 9, no. 3, pp. 211-222, 1998.

[15] D. Hoffman, G. Fernando, V. Goyal, and M. Civanlar, "RTP payload format for MPEG1/MPEG2 video," Internet Engineering Task Force, RFC 2250, January 1998.

[16] K. Van der Wal, M. Mandjes, and H. Bastiaansen, "Delay performance analysis of the new internet services with guaranteed QoS," *Proc. IEEE*, vol. 85, no. 12, pp. 1947-1957, December 1997.

[17] H. Naser and A. Leon-Gracia, "Performance evaluation of MPEG2 video using guaranteed service over IP-ATM networks," *Multimedia Computing and Systems Conference*, Austin, Texas, USA, June 28 – July 1, 1998.

[18] R. Braden, L. Zhang, S. Berson, S. Herzog, and S. Jamin, "Resource ReSerVation Protocol (RSVP) – Version 1 functional specification," Internet Engineering Task Force, RFC 2205, September 1997.

[19] L. Georgiadis, R. Guerin, V. Peris, and R. Rajan, "Efficient support of delay and rate guarantees in an internet," *Comp. Comm. Rev.*, vol. 26, no. 4, pp. 106-116, October 1996.

[20] M. F. Alam, M. Atiquzzaman, and M. A. Karim, "Traffic shaping for MPEG video transmission over Guaranteed Service on the Internet," to be presented at *1999 IEEE Global Communications Conference*, Rio de Janeiro, Brazil, December 5-9, 1999.

[21] O. Rose, "Statistical properties of MPEG video traffic and their impact on traffic modeling in ATM systems," Report No. 101, Institute of Computer Science, University of Würzberg, February 1995.